CHINESE OPTICS LETTERS

Vol. 20, No. 8 | August 2022

Dynamics of multi-state in a simplified mode-locked Yb-doped fiber laser

Zexin Zhang (张泽新), Jinrong Tian (田金荣)*, Youshuo Cui (崔友硕), Yunfeng Wu (吴云峰), and Yanrong Song (宋晏蓉)**

School of Physics and Optoelectronics, Faculty of Science, Beijing University of Technology, Beijing 100124, China

*Corresponding author: jrtian@bjut.edu.cn

**Corresponding author: yrsong@bjut.edu.cn

Received February 10, 2022 | Accepted April 28, 2022 | Posted Online May 26, 2022

The dispersive Fourier transform technique provides feasibility of exploring non-repetitive events and the buildup process in ultrafast lasers. In this paper, we report a new buildup process of dissipative solitons in a simplified mode-locked Yb-doped fiber laser, which includes more complex physics stages such as the *Q*-switching stage, raised and damped relaxation oscillation stages, noise-like stage, successive soliton explosions stage, and soliton breathing stage. Complete evolution dynamics of noise-like pulse and double pulse are also investigated with dispersive Fourier transform. For the noise-like pulse dynamics process, it will only experience the *Q*-switching and relaxation oscillation stages. In the case of dissipative soliton and noise-like pulse, the double pulse buildup behavior is manifested as the replication of individual pulses. A weak energy migration occurs between two pulses before reaching steady state. Meanwhile, real-time mutual conversion of the dissipative soliton and noise-like pulse has been experimentally observed, which appears to be instantaneous without extra physical processes. To the best of our knowledge, this is the first report on these physical phenomena observed together in a mode-locked fiber laser. The results further enrich the dynamics of mode-locked fiber lasers and provide potential conditions for obtaining intelligent mode-locked lasers with controllable output.

Keywords: dispersive Fourier transform; dynamics process; simplified mode-locked fiber lasers; dissipative soliton; noise-like pulse; double-pulse.

DOI: 10.3788/COL202220.081402

1. Introduction

Mode-locked fiber lasers have attracted extensive interest for their applications in optical communications, micro-processing, biomedical imaging, and other fields[1–4]. With the maturity of fiber manufacturing technology and the continuous deepening of research, fiber lasers have made major breakthroughs in high peak power[5–7], narrow pulse[8–10], and broad spectrum[11]. The output state has also become diversified, e.g., dissipative soliton (DS)[12–14], noise-like pulse (NLP)[14,15], DS resonance (DSR)[16,17], etc. However, limited by conventional instruments, real-time observation of laser output cannot be carried out instead of multiple averages[1,18]. Furthermore, dynamics of mode-locking formation is quite difficult to detect for the existence of transient phenomena, which raises a severe obstacle to clarifying the mode-locking process in fiber lasers.

This limitation can be circumvented by using the time-stretch dispersive Fourier transform (TS-DFT) technique to some extent[19,20], which maps the spectral information to the time domain with a suitable oscilloscope and photodetector, and thus real-time measurement of the pulse spectrum can be realized. With the dispersive Fourier transform (DFT) technique, transient soliton dynamics has been revealed and verified experimentally in recent years, for instance, the process of establishing the steady-state soliton molecules[20–22], soliton collision[23–25], and multi-pulse soliton interactions[26–29]. In addition, the buildup dynamics of DS has also been studied to a certain extent[30–33]. Several of the aforementioned references have shown that the spectrum broadens in a short time with rapid increase of intra-cavity energy during the DS buildup. Since the balance among gain, loss, dispersion, and nonlinear effects has not yet been reached, spectrum fluctuations can be observed before the formation of stable DSs. Moreover, the relaxation oscillations (ROs) and noise-like phenomena have not been observed throughout the process in the normal dispersion regime. However, compared to other behaviors in the laser, the buildup process of DS does not include a lot of stages. For NLP[34], the entire buildup dynamics process has not yet been discovered. Meanwhile, the mutual exchanging process between two kinds of solitons has not been reported.

In this work, we demonstrate the observation of the buildup dynamics process of multiple states in a simplified mode-locked

Yb-doped fiber (YDF) laser by TS-DFT. Rotating the angle of the polarized beam splitter (PBS), the only spatial element in the cavity, DS, NLP, and double pulse (DP) can be generated in the laser. The fast pass and stop of mode locking are achieved by placing a chopper inside the cavity different from previous reports. Compared with previously reported buildup process of stable DS, our measurements reveal complex dynamics at the birth of DS, e.g., *Q*-switching (QS), raised and damped ROs, noise-like state, successive soliton explosions, and soliton breathing. In the case of NLP, it will only experience the process of QS and RO. Considering the buildup of DP, whether in DS or NLP, the overall performance is the replicate of single pulse, and weak energy migration occurs between the two pulses before reaching steady state. Furthermore, the experimental result also reveals the inter-conversion of the NLP and DS for the first time, to the best of our knowledge.

2. Experimental Setup

The experimental setup is depicted in Fig. 1, which includes a simplified mode-locked fiber laser and a DFT system. Figure 1(a) shows the nonlinear polarization rotation (NPR) mode-locked YDF laser pumped by a 980 nm laser diode with output power up to 620 mW. The pump light is coupled into the cavity through a wavelength division multiplexer (WDM) of 980/1030 nm. The gain fiber is a piece of YDF with a length of 25 cm. A 30% output coupler (OC) is used to extract pulses from the cavity and the optical isolator (ISO) forces unidirectional operation. Two collimators (C1 and C2) allow laser transmission in the space, cooperating with the PBS to achieve NPR mode locking. The total cavity length is 2.65 m with net cavity dispersion of 0.056 ps^2. In the fiber laser, a mechanical chopper is placed between C1 and C2 to switch the laser on and off, so as to facilitate successive measurements of the dynamics process of a pulse with DFT. The DFT system is illustrated in Fig. 1(b). An 8 km single-mode fiber (SMF-28e) is used to stretch the soliton in the time domain, which generates an approximate dispersion of 178 ps^2 near 1 μm. The time-averaged spectrum and real-time temporal information are determined by an optical spectrum analyzer (OSA) and a 6 GHz oscilloscope with a 12.5 GHz bandwidth photodetector, respectively. Other information of laser pulse can be obtained by a frequency spectrum analyzer and an autocorrelator before DFT. The resolution of the DFT system is calculated to be 0.25 nm.

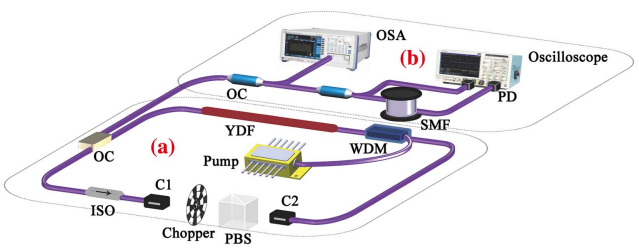

Fig. 1. Schematic of the experimental setup. (a) Simplified NPR mode-locked Yb-doped fiber laser. (b) DFT system. WDM, wavelength division multiplexer; YDF, Yb-doped fiber; OC, output coupler; ISO, isolator; PBS, polarized beam splitter; C1, C2, collimators; PD, photodetector.

3. Results and Discussion

By applying constant stress to the gain fiber, self-starting mode locking is readily obtained for the laser. In the experiment, we put a cylindrical iron block on the gain fiber to produce the necessary stress. The laser can bring about DS and NLP pulses with pump thresholds of 380 mW and 290 mW, respectively. When the pump power meets both requirements of DS and NLP, the transition between the DS and NLP can be obtained by tuning the tilt angles of the PBS from −5° to 5°, and the accompanying transition of mode-locking states is shown in Fig. 2.

Figure 3 demonstrates the output characteristics of DS and NLP at a pump power of 560 mW. The spectrum of DS has a 3 dB spectral bandwidth of 8.4 nm centered at 1029 nm, and the corresponding pulse duration is 9.84 ps (assuming a Gaussian pulse shape). The spectrum of NLP has an equivalent 3 dB bandwidth, and the corresponding spectral coverage is slightly increased. Moreover, the autocorrelation trace presents a pedestal width of 14.43 ps and a spike of 255.1 fs, which confirms that it is an NLP.

In order to facilitate the subsequent buildup process of the pulse, we first measure stable DS pulses with DFT. The last frame of the spectrum in the real-time series of DS is displayed in Fig. 4(a), and the inset figure shows the entire evolution process. A single frame of the DS's spectrum has two steep edges. A comparison of Figs. 3(a) and 4(a) indicates that the spectrum derived from DFT agrees well with the counterpart from the OSA except for the spectral inversion due to dispersion and some slight differences caused by the inherent noise of the oscilloscope, which implies that the spectral information is accurately mapped to the time domain.

To further prove this fact, the above mapping relationship can be expressed as

$$\Delta t = |D| L \Delta\lambda, \tag{1}$$

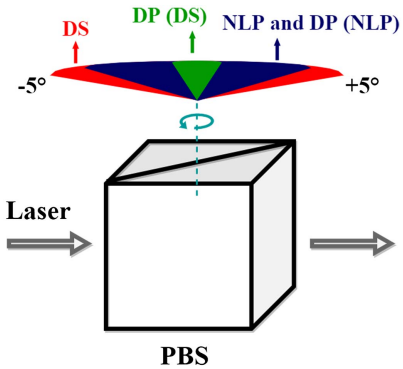

Fig. 2. Corresponding mode-locking states at different tilt angles of PBS in the cavity (±5°).

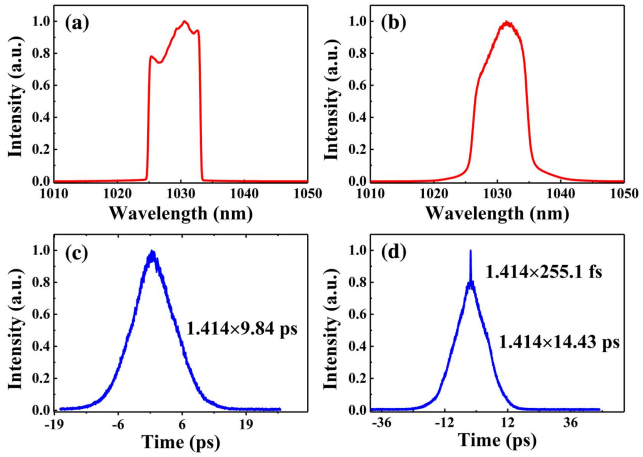

Fig. 3. Output characteristics of DS and NLP at a pump power of 560 mW. (a) Spectrum of DS. (b) Spectrum of NLP. (c) and (d) show the autocorrelation traces corresponding to (a) and (b), respectively.

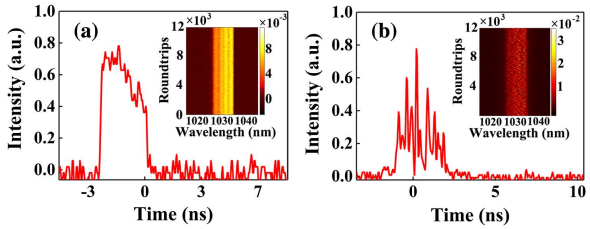

Fig. 4. Last frame of the spectrum of (a) DS and (b) NLP in the real-time sequences measured with the DFT technique. Inset: the entire evolution process.

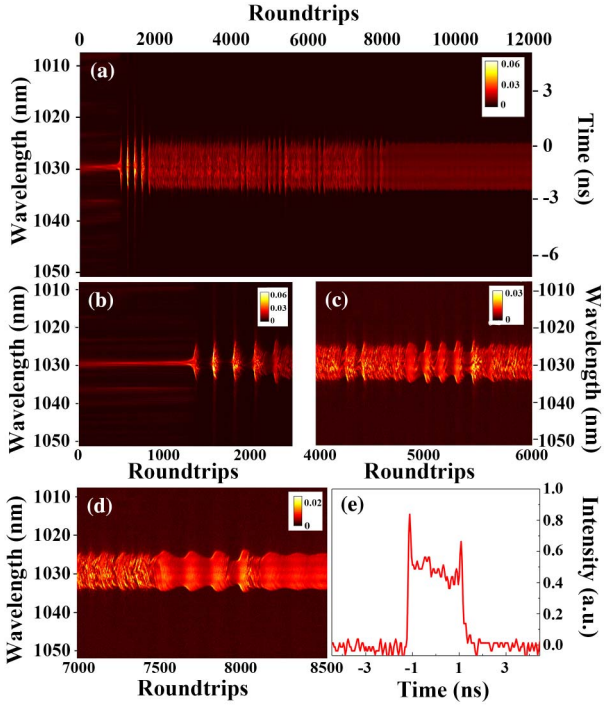

Fig. 5. Real-time spectral evolution during the formation of DS. (a) Entire buildup dynamics process. (b) 0–2500 round trips in (a), which contains the QS and RO processes. (c) Successive soliton explosions during 4000–6000 round trips in (a). (d) Soliton breathing and soliton explosion in the final stage of buildup stable DS. (e) Single-frame spectrum derived from 7500 round trips in (a).

where $\Delta\lambda$ is the spectral bandwidth, Δt is the time spacing after DFT, D and L are the dispersion parameter and length of the SMF, respectively. Since D is about $-40\ \mathrm{ps/(nm \cdot km)}$ and $L = 8$ km in the experiments, the above relationship can be expressed as $\Delta t = (0.32\ \mathrm{ns/nm}) \times \Delta\lambda$. The spectral width of DS is 8.4 nm, and the temporal width after mapping is about 2.7 ns. For NLP, we carry out the same processing, and Fig. 4(b) shows the result. Different from DS, the temporal profile displays a noise-like structure (the envelope has many sub-pulses with random amplitude) after passing the DFT device, which is in accordance with the characteristics of an NLP. Although the single-frame spectrum exhibits the above characteristics, the corresponding temporal width is about 2.7 ns for the NLP. Obviously, the experimental results are consistent with the above theoretical relationship [Eq. (1)], which demonstrates the validity of the experiment.

3.1. Buildup dynamics process of DS

The entire buildup dynamics process of DS is shown in Fig. 5(a). With a proper rotation speed of the chopper, this result can be easily obtained in experiment. Different from previously reported work, the buildup dynamics process of DS consists of more physical processes. Figure 5(b) demonstrates that weak QS occurs at the initiation of pulse formation, and the intra-cavity energy is stored in the main pulse. With more round trips, the main pulse splits and absorbs the energy of the adjacent pulses to form a wider temporal signal, which is the preliminary establishment of the mode-locking spectrum. The raised and damped RO appears in the following time. Since the energy of the main pulse in the QS stage has accumulated to a certain high level, the raised RO has a shorter interaction time than the damped RO in the cavity. The coexistence of both two states is a novel phenomenon that has not been reported. The raised RO is caused by insufficient gain of the fiber laser at the initial stage of operation and input pump energy far exceeding the mode-locking threshold. The incomplete interaction between the pump light and the gain fiber makes the laser pulse start the next process before reaching the actual peak. With the pulse energy approaching the tolerable peak in the cavity, due to the constant balance of pump excitation and stimulated radiation, the damped RO stage occurs in the next process. Whether raised RO or damped RO is essentially caused by the sharp changes in the intra-cavity photon density and inversion population.

In the experiment, the randomly fluctuating spectral spikes in raised RO spread out along both sides to form the initial spectral profile. Along with the decrease and redistribution of light pulse energy in the damped RO, the quasi-stable mode-locked pulse is established and evolves, as shown in Fig. 5(a) approximately

from 1900 to 8400 round trips, and more detailed information is depicted in Figs. 5(c) and 5(d). Most round trips in quasi-steady-state mode locking are similar to the stable NLP process in Fig. 4(b). Figure 5(c) shows the successive soliton explosions at certain pump powers. The main characteristics of solitons in this state are the structural collapse of the spectrum and the periodic operation, which is essentially different from the NLP regime. After 7500 round trips in Fig. 5(a), two steep edges of the DS spectrum have formed, as shown in Fig. 5(e). Since the pulse propagates in the simplified cavity without wave plates, filters, etc., it has to rely on its own breathing to form the final stable DS spectrum. Figure 5(d) reveals the soliton breathing and soliton explosion in the final stage of stable DS buildup. During the entire dynamics process, soliton explosions happen randomly, which may occur at any time after RO and before DS. The results reveal a more complex physical process of DS formation and further enrich the soliton dynamics in fiber lasers, which offers the possibility of obtaining a controllable laser.

3.2. Buildup dynamics process of NLP

Figure 6(a) shows the whole buildup dynamics process for an NLP; the raised and damped ROs also exist in this process. The energy of the main pulse increases rapidly close to the peak at the end of QS, and, as a result, the raised RO of the NLP looks not as obvious as that of DS. It is worth noting that the formed NLP spectrum has an irregular shape, which includes a large envelope containing many sub-pulses with random fluctuations in intensity [Fig. 6(b)]. It agrees with the physical definition of NLP and differs from the soliton regime. To better understand

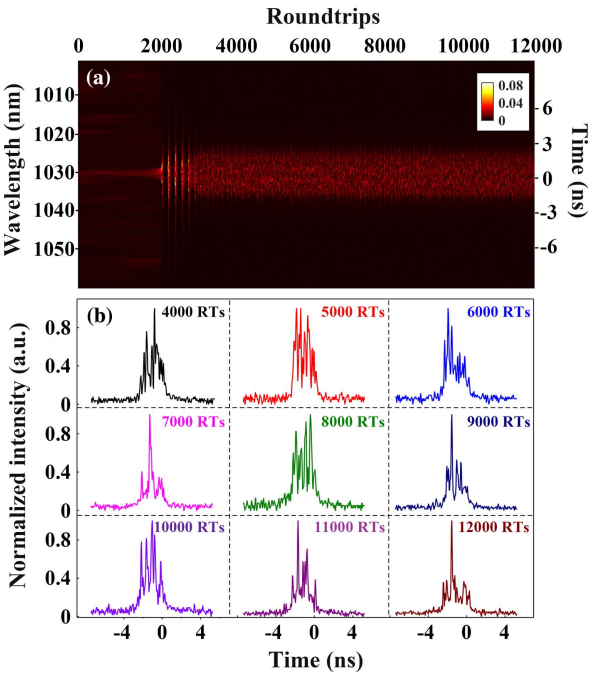

Fig. 6. Real-time spectral evolution dynamics during the formation of NLP. (a) Entire buildup dynamics process. (b) The NLP spectrum after different round trips (RTs) in an evolution period.

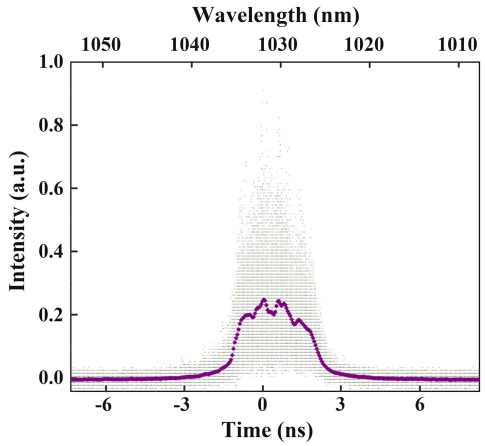

Fig. 7. Ensemble average of the spectra within the last 500 round trips in Fig. 6(a).

this, we performed an ensemble average of spectra within the last 500 round trips in Fig. 6(a), and the result is shown in Fig. 7. It can be seen that the ensemble-averaged spectrum (purple curve in Fig. 7) is quite similar to the spectrum directly measured by the OSA [Fig. 3(b)], even though the shape and intensity of each frame of the spectrum are different (the scatterplot in Fig. 7). The fine peak structure in a single frame of the spectrum is replaced by the overall smooth spectral density. This result confirms that the smooth spectrum for NLP shown in OSA arises indeed from the ensemble averaging of highly structured and fluctuating elementary spectra, which provides a unique insight into the buildup dynamics and composition mechanism of an NLP and implies a new method of identifying an NLP.

3.3. Buildup dynamics process of DP (depending on DS and NLP)

When the intra-cavity nonlinearity is strong enough, multiple pulses are often generated. In past years, researchers have focused more on the "multi-soliton modes" generated by multi-pulse interactions, such as soliton molecules and soliton rain. For the first time, to the best of our knowledge, we detect the birth dynamics process of a double DS pulse with different energies using DFT, and Fig. 8(a) shows the results. The appearance of QS and RO in the early stages of evolution is shown in Fig. 8(b). The two mode-locked pulses occur at the position of local maximum energy and absorb the energy of adjacent pulses to realize rapid spectral broadening between QS and RO. The raised and damped RO gives rise to a rapid increase in energy for the main pulse (with higher energy), and then the energy decreases to a level capable of sustaining the metastable oscillation. Due to the gain competition in the cavity, only the damped RO exists in the formation of the sub-pulse. Different from the single-pulse evolution [Fig. 5(b)], the RO of DP is not continuous, and the sub-pulse needs to maintain its own oscillation by exchanging energy with the main pulse through non-primary RO. The result between 2000 and 10,000 round trips in Fig. 8(a) shows the NLP phenomenon. It can be found that small pulses

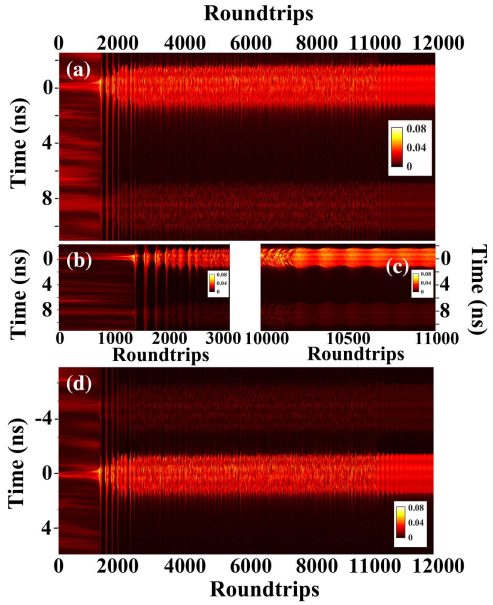

Fig. 8. Real-time spectral evolution dynamics during the formation of DP (for DS). (a) The birth dynamics process of DP. (b) QS and RO in the early stages of evolution for (a). (c) Soliton breathing in dynamics process. (d) The birth dynamics process of coexisting sub-pulse and adjacent main pulse.

have been wandering between the two pulses [sub-pulse with the next main pulse, Fig. 8(d)] for energy exchange and spectral overlap, which effectively avoids the soliton explosion during the pulse buildup process. The soliton breathing is demonstrated in Fig. 8(c), which is derived from the result between 10,000 and 11,000 round trips in Fig. 8(a). Strong breathing makes the pulse energy well concentrated in a certain range. On further weakening of the breathing effect, the mode locking gradually becomes stable. On the whole, the behavior of two pulses displays a high degree of consistency.

The buildup dynamics process of the double NLP pulse is shown in Fig. 9(a). The inherent characteristics of NLP and the mode-locked pulse in the QS phase have accumulated enough energy, so the subsequent RO only lasts for a short time. The wide spectrum of NLP also enables the exchange between two pulses without destroying the stability of the overall structure. At the same time, the tight connection between two pulses [sub-pulse with next main pulse, Fig. 9(b)] allows for the absence of intermittent RO during the process. The experimental results also reveal that the main pulse always guides the sub-pulse to follow the same procedure during the evolution of DP. Before reaching the steady state, two pulses always share phase information and energy in the form of small pulses.

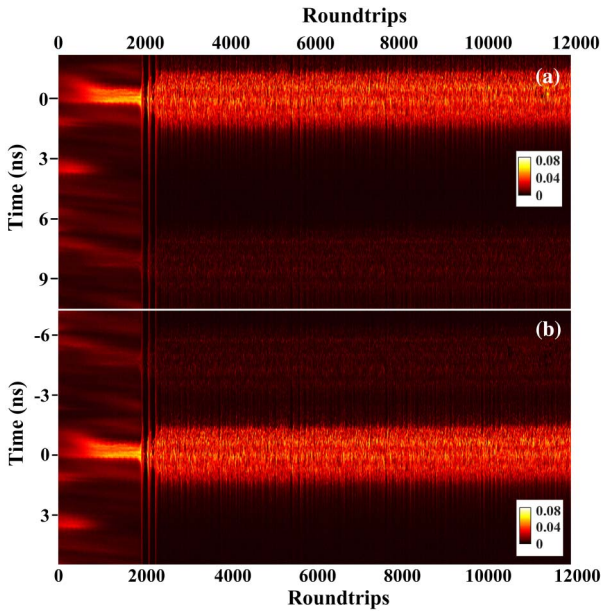

Fig. 9. Real-time spectral evolution dynamics during the formation of DP (for NLP). (a) The DP birth dynamics process of NLP. (b) The birth dynamics process of the sub-pulse with the next main pulse.

3.4. Dynamics process of the conversion between DS and NLP

As two typical mode-locking states, DS and NLP are readily obtained in fiber lasers. There have been many reports contributed to the mechanisms of both DS and NLP independently. However, the real-time diagnosis of the conversion of DS and NLP in a fiber laser is seldom reported.

Here, we report the first observation, to the best of our knowledge, of the entire conversion process of DS and NLP in a mode-locked laser with the aid of DFT. The conversion processes of DS to NLP and NLP to DS are shown in Figs. 10(a) and 10(b), respectively, in which it can be seen that the transition between the two steady-state mode locking is accompanied by a sudden change in energy at a critical point and without other physical processes. The maximum energy of NLP is considerably higher than that of DS. Compared with the DS buildup dynamics

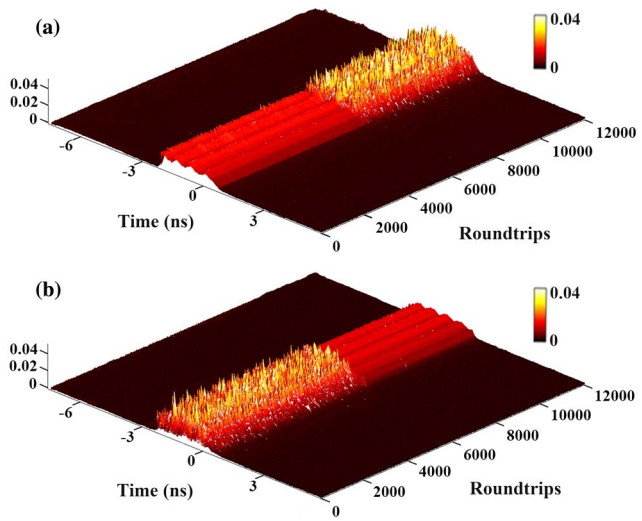

Fig. 10. Entire inter-conversion process of DS and NLP. (a) Conversion from DS to NLP. (b) Conversion from NLP to DS.

process, the above conversion process does not rely on soliton breathing for the step-by-step jump in energy unlike the evolution from non-stationary to steady-state. Moreover, the diagnosis of other transient behaviors in mode-locked fiber lasers can be carried out with the same method.

3.5. Discussion

It is noteworthy that the abovementioned results are obtained in a simplified mode-locked fiber laser. Rotating the PBS angle is equivalent to modulating the instantaneous power of the pulse. Different instantaneous powers cause the pulses to operate in different saturated absorption regions[35], which indicates that the laser can output different types of pulses by changing the tilt angle of the PBS. The spectral information is mapped to time domain by means of DFT, combined with mechanical chopping, and the corresponding dynamics processes can be revealed experimentally. Different from the conventional structures, the cavity has only one PBS for polarization control, in spite of which the laser still operates in NPR mode locking. Such a cavity design leads to an adaptive evolution of the pulse in the fiber, which plays an important role in the mode locking. In other words, the mode-locked pulse requires more physical processes to achieve the transition from the start to steady state. The spectrum broadens rapidly in the late QS stage, which is attributed to the character of saturable absorption in NPR mode locking. Similar memory behavior occurs in the experiment (from Ref. [21]); pulses with local maxima in power can evolve into the final mode-locked pulses, while pulses with the highest power dominate the evolution.

Since the chopper is placed inside the cavity, the operation will turn on and off both for the power and in-progress state, which allows the RO stage to occur after the QS, and the sustaining time of RO is relatively short compared with previous reports. Limited by the unsaturated absorption of pump energy in the gain fiber and the energy tolerance of the cavity to the oscillation pulse, the evolution process requires raised RO and damped RO to complete the redistribution of energy and thus achieve quasi-steady-state mode locking. An interesting phenomenon in this experiment is that the majority of pulse energy in the QS stage directly affects the sustaining time of RO during the process. A higher pulse energy in the QS stage leads to a shorter sustaining time of RO. At the same time, high pulse energy increases the peak power of the mode-locked pulse, which makes the final output pulse tend to be an NLP. This character brings a new perspective in optimizing the laser output.

The high pulse energy of an NLP makes it appear earlier after the RO and occupy most of the round trips during the evolution (more than half of the entire process), which explains why an NLP is easily obtained in mode locking. With a suitable balance among gain, loss, nonlinearity, and dispersion, the pulse can eventually evolve into a stable DS. However, quite a few factors may affect the final state of the mode-locked pulse, e.g., the round-trip loss affects whether the output is DS or NLP; the magnitude of nonlinearity determines whether the output is multi-pulse, etc. However, no matter what the final state is, the NLP state would exist definitely during the evolution.

4. Conclusion

In summary, we have experimentally demonstrated the buildup dynamics processes of multiple states by DFT in a simplified NPR fiber laser, where only a PBS is used for polarizing control. The fast pass and stop of mode locking are achieved by placing a chopper inside the cavity different from previous reports. On these conditions, a new and complex buildup dynamics process of DS is revealed with more physical stages, e.g., QS, raised and damped ROs, noise-like state, successive soliton explosions, and soliton breathing. For the dynamics process of NLP, it will only experience the QS and the RO. Compared with DS, the buildup time of stable NLP is much shorter, which is consistent with the fact that it is easier to obtain NLP in experiments. At the same time, due to their own characteristics, soliton breathing and soliton explosion will not appear in the evolution process of NLP. The dynamics process of DP can be obtained experimentally by optimizing the resonator losses. In the context of DS and NLP, the buildup behavior of DP is substantially the same as the single pulse. A weak energy migration occurs between two pulses before reaching a steady state, which effectively prevents soliton explosion throughout the process. The experiment also reveals the inter-conversion of the NLP and DS for the first time, to the best of our knowledge, which appears to be an instantaneous conversion rather than other extra physical processes. These results further enrich the dynamics of mode locking in fiber lasers and provide potential conditions for obtaining intelligent mode-locked lasers with controllable output.

Acknowledgement

This work was supported by the Beijing Natural Science Foundation (No. 4192015) and the National Natural Science Foundation of China (No. 61975003).

References

1. U. Keller, "Recent developments in compact ultrafast lasers," Nature **424**, 831 (2003).
2. C. Xu and F. W. Wise, "Recent advances in fibre lasers for nonlinear microscopy," Nat. Photonics **7**, 875 (2013).
3. C. W. Freudiger, W. Yan, G. R. Holtom, N. Peyghambarian, X. S. Xie, and K. Q. Kieu, "Stimulated Raman scattering microscopy with a robust fibre laser source," Nat. Photonics **8**, 153 (2014).
4. S. T. Sanders, "Wavelength-agile fiber laser using group-velocity dispersion of pulsed super-continua and application to broadband absorption spectroscopy," Appl. Phys. B **75**, 799 (2002).
5. Z. W. Liu, Z. M. Ziegler, L. G. Wright, and F. W. Wise, "Megawatt peak power from a Mamyshev oscillator," Optica **4**, 649 (2017).
6. S. Pavel, W. Fu, L. G. Wright, O. Michel, and F. W. Wise, "Self-seeded, multi-megawatt, Mamyshev oscillator," Opt. Lett. **43**, 2672 (2018).
7. R. C. Lu, H. Teng, J. F. Zhu, Y. Yu, W. Liu, G. Q. Chang, and Z. Y. Wei, "High power Yb-fiber laser amplifier based on nonlinear chirped-pulse amplification at a repetition rate of 1 MHz," Chin. Opt. Lett. **19**, 091401 (2021).

8. X. Y. Zhou, D. Yoshitomi, Y. Kobayashi, and T. Kenji, "Generation of 28-fs pulses from a mode-locked ytterbium fiber oscillator," Opt. Express **16**, 7055 (2008).
9. X. H. Li, J. J. Feng, W. J. Mao, Y. Feng, and J. Jiang, "Emerging uniform Cu_2O nanocubes for 251st harmonic ultrashort pulse generation," J. Mater. Chem. C **8**, 14386 (2020).
10. R. Q. Xu, J. R. Tian, and Y. R. Song, "Noise-like pulses with a 14.5 fs spike generated in an Yb-doped fiber nonlinear amplifier," Opt. Lett. **43**, 1910 (2018).
11. H. Chen, S. Chen, Z. F. Jiang, and J. Hou, "0.4 μJ, 7 kW ultrabroadband noise-like pulse direct generation from an all-fiber dumbbell-shaped laser," Opt. Lett. **40**, 5490 (2015).
12. L. M. Zhao, D. Y. Tang, X. Wu, and H. Zhang, "Dissipative soliton generation in Yb-fiber laser with an invisible intracavity band pass filter," Opt. Lett. **35**, 2756 (2010).
13. T. Chai, X. H. Li, T. C. Feng, P. L. Guo, Y. F. Song, Y. X. Chen, and H. Zhang, "Few-layer bismuthene for ultrashort pulse generation in dissipative system based on evanescent field," Nanoscale **10**, 17617 (2018).
14. Z. X. Zhang, J. R. Tian, C. X. Xu, R. Q. Xu, Y. S. Cui, B. H. Zhuang, and Y. R. Song, "Noise-like pulse with a 690 fs pedestal generated from a nonlinear Yb-doped fiber amplification system," Chin. Opt. Lett. **18**, 121403 (2020).
15. M. Horowitz, Y. Barad, and Y. Silberberg, "Noise like pulses with a broadband spectrum generated from an erbium-doped fiber laser," Opt. Lett. **22**, 799 (1997).
16. X. Wu, D. Y. Tang, H. Zhang, and L. M. Zhao, "Dissipative soliton resonance in an all-normal dispersion erbium-doped fiber laser," Opt. Express **17**, 5580 (2009).
17. Y. F. Wu, J. R. Tian, Z. K. Dong, C. B. Liang, and Y. R. Song, "Generation of two dissipative soliton resonance pulses in an all-anomalous-dispersion regime thulium-doped fiber laser," IEEE Photonics J. **11**, 99 (2019).
18. H. Li, D. G. Ouzounov, and F. W. Wise, "Starting dynamics of dissipative-soliton fiber laser," Opt. Lett. **35**, 2403 (2010).
19. K. Goda and B. Jalali, "Dispersive Fourier transformation for fast continuous single-shot measurements," Nat. Photonics **7**, 102 (2013).
20. G. Herink, F. Kurtz, B. Jalali, D. R. Solli, and C. Ropers, "Real-time spectral interferometry probes the internal dynamics of femtosecond soliton molecules," Science **356**, 50 (2017).
21. X. M. Liu, X. K. Yao, and Y. D. Cui, "Real-time observation of the buildup of soliton molecules," Phys. Rev. Lett. **121**, 023905 (2018).
22. K. Krupa, K. Nithyanandan, U. Andral, P. Tchofo-Dinda, and P. Grelu, "Real-time observation of internal motion within ultrafast dissipative optical soliton molecules," Phys. Rev. Lett. **118**, 243901 (2017).
23. A. F. J. Runge, N. G. R. Broderick, and M. Erkintalo, "Observation of soliton explosions in a passively mode-locked fiber laser," Optica **2**, 36 (2015).
24. M. Liu, A. P. Luo, Y. R. Yan, S. Hu, Y. C. Liu, C. Hu, Z. C. Luo, and W. C. Xu, "Successive soliton explosions in an ultrafast fiber laser," Opt. Lett. **41**, 1181 (2016).
25. Y. Yu, Z. C. Luo, J. Kang, and K. K. Y. Wong, "Mutually ignited soliton explosions in a fiber laser," Opt. Lett. **43**, 4132 (2018).
26. Y. Yu, B. Li, X. M. Wei, Y. Q. Xu, K. K. M. Tsia, and K. K. Y. Wong, "Spectral-temporal dynamics of multipulse mode-locking," Appl. Phys. Lett. **110**, 201107 (2017).
27. G. M. Wang, G. W. Chen, W. L. Li, C. Zeng, and H. R. Yang, "Decaying evolution dynamics of double-pulse mode-locking," Photon. Res. **6**, 825 (2018).
28. J. S. Peng and H. P. Zeng, "Build-up of dissipative optical soliton molecules via diverse soliton interactions," Laser Photonics Rev. **12**, 1800009 (2018).
29. Y. Q. Wang, X. Y. Wang, J. S. Peng, M. Yan, K. Huang, and H. P. Zeng, "Experimental observation of transient mode-locking in the build-up stage of a soliton fiber laser," Chin. Opt. Lett. **19**, 071401 (2021).
30. H. J. Chen, M. Liu, Y. Jian, S. Hu, J. B. He, A. P. Luo, W. C. Xu, and Z. C. Luo, "Buildup dynamics of dissipative soliton in an ultrafast fiber laser with net-normal dispersion," Opt. Express **26**, 2972 (2018).
31. J. S. Peng, S. Mariia, S. Srikanth, T. Nikita, D. V. Churkin, S. K. Turitsyn, and H. P. Zeng, "Real-time observation of dissipative soliton formation in nonlinear polarization rotation mode-locked fibre lasers," Commun. Phys. **1**, 20 (2018).
32. P. Ryczkowski, M. Nrhi, C. Billet, J. M. Merolla, G. Genty, and J. M. Dudley, "Real-time full-field characterization of transient dissipative soliton dynamics in a mode-locked laser," Nat. Photonics **12**, 221 (2018).
33. Y. D. Cui and X. M. Liu, "Revelation of the birth and extinction dynamics of solitons in SWNT-mode-locked fiber lasers," Photon. Res. **7**, 423 (2019).
34. A. F. J. Runge, C. Aguergaray, N. G. R. Broderick, and M. Erkintalo, "Coherence and shot-to-shot spectral fluctuations in noise-like ultrafast fiber lasers," Opt. Lett. **38**, 4327 (2013).
35. R. Q. Xu, Y. R. Song, Z. K. Dong, K. X. Li, and J. R. Tian, "Compact Yb-doped mode-locked fiber laser with only one polarized beam splitter," Appl. Opt. **56**, 1674 (2017).